Synergistic Mechanical Enhancement in a Novel Hybrid Sawdust/Coir-Reinforced Epoxy Composite Bars: A Sustainable Material for Structural Applications

Daerefa-a Mitsheal Amafabia[1*], Sotonte Emmanuel Jack[2]

[1]Senior Lecturer, Department of Mechanical Engineering, Rivers State University, Port Harcourt, Rivers State, Nigeria.
[2]Lecturer II, Department of Mechanical Engineering, Rivers State University, Port Harcourt, Rivers State, Nigeria.
*Corresponding Author

(Received: 11.05.2026; Accepted: 19.06.2026)

Abstract

The integration of industrial and agricultural waste into high-value composites is a cornerstone of the circular economy. This study presents a comprehensive investigation into the mechanical properties and reinforcing mechanisms of a novel hybrid composite bar utilizing sawdust (SW) and coir fibre (CF) as reinforcements in an epoxy matrix. Four composite specimens were fabricated with varying reinforcement ratios: equal fibre blend (65% resin, 15% sawdust, 15% coir), coir-dominant (65% resin, 25% coir, 10% sawdust), sawdust-dominant (65% resin, 25% sawdust, 10% coir), and high-fibre content (60% resin, 20% sawdust, 20% coir). Mechanical tests, including tensile strength, Charpy impact resistance, and microstructural analysis, were conducted using a Universal Testing Machine, a Charpy impact testing machine, and metallography microscopy, respectively, in accordance with ASTM standards. Results showed that the coir-dominant specimen exhibited the highest ultimate tensile strength (19 MPa), while the equal fibre blend achieved the highest average impact resistance (2.18 J). The sawdust-dominant specimen recorded the lowest tensile strength (12 MPa), indicating weaker fibre-matrix bonding. Microstructural analysis revealed that uniform fibre distribution and effective resin penetration enhance mechanical performance, while voids and particle debonding limit it. These findings confirm that sawdust/coir-epoxy composite bars are viable for applications such as furniture, packaging, and low-cost structural components, contributing to waste valorisation and sustainability.

Keywords: *Charpy impact resistance; Coconut coir; Eco-friendly composites; Epoxy matrix; Hybrid composite bars; Microstructural analysis; Natural fibre composites; Sawdust; Tensile strength*

HIGHLIGHTS

- Study investigates the synergistic mechanical performance of a novel hybrid sawdust/coir-reinforced epoxy composite bar for sustainable structural applications.
- Four composite specimens with varying reinforcement ratios were fabricated and subjected to standardised ASTM tensile, Charpy impact resistance, and microstructural analyses.
- The coir-dominant specimen achieved the highest tensile strength (19 MPa); the equal-fibre-blend specimen exhibited the greatest average impact energy absorption (2.18 J).
- The study establishes the novelty of utilising co-reinforcement of locally sourced sawdust and coconut coir in an epoxy matrix as an eco-friendly alternative to synthetic composites.

INTRODUCTION

The increasing global demand for sustainable and eco-friendly materials has driven research into alternative resources that can replace conventional materials in construction, manufacturing, and composite production (Gibson, 2016; Singh *et al.*, 2026). Natural fibres and agricultural by-products such as sawdust and coconut coir have gained significant attention due to their abundance, renewability, and potential to reduce environmental degradation. These materials, often considered waste products, hold untapped potential for creating cost-effective, lightweight, and environmentally friendly composites with desirable mechanical properties (Mallick, 2007; Uchendu *et al.*, 2026).

Sawdust, a by-product of woodworking processes, is generated in large quantities across furniture manufacturing, sawmills, and construction industries. Its lignocellulosic composition (cellulose, hemicellulose, and lignin), lightweight nature, biodegradability, and low cost make it a viable candidate for composite reinforcement. Despite these advantages, the mechanical performance of sawdust—particularly when combined with other natural fibres—requires systematic investigation (Soutis, 2005).

Coconut coir, derived from coconut husks and abundant in tropical regions, is noted for its durability, moisture resistance, and high lignin content that contributes to its inherent toughness. Unlike synthetic fibres such as glass or carbon, coir is biodegradable and poses minimal environmental risks. The combination of sawdust and coir in a composite bar presents an opportunity to harness their complementary properties: sawdust provides a fine particulate filler effect while coir contributes tensile reinforcement and flexibility, with the potential to synergistically improve the overall mechanical performance (Daniel and Ishai, 2006).

Prakash *et al.* (2020) demonstrated that coconut shell and coconut fibre enhance the mechanical properties of concrete, while Tawasil *et al.* (2021) found that hybrid sawdust–coir particleboards satisfied BS EN 312:2010 standards with a modulus of elasticity of 1510 N/mm². Oladele *et al.* (2020) reported a tensile strength of 25 MPa and flexural strength of 38 MPa for hybrid sawdust–coir composites in a polyester matrix, outperforming single-material composites. Gurusamy *et al.* (2024) found that tensile and compressive strengths improved consistently up to 50% filler loading in Malabar Ironwood sawdust–COCO dust hybrid composites. Bui *et al.* (2020) reported untreated coir tensile strengths of 15–25 MPa, enhanced after NaOH treatment, while Hasan *et al.* (2020) found alkali treatment increased composite tensile strength by approximately 15% to reach 31 MPa.

A notable research gap exists regarding the systematic evaluation of hybrid sawdust–coir bars fabricated using hand lay-up in an epoxy matrix, with concurrent tensile, impact, and microstructural characterisation of multiple formulations. This study aims to fill this gap, with the objective of experimentally evaluating the mechanical properties of four sawdust/coir-epoxy composite bar formulations for potential use in furniture, packaging, and low-cost structural applications.

MATERIALS AND METHODS

Materials

The composite bars were fabricated using the following constituents (Fig. 1):

(i) *Sawdust*—fine, dry particles sieved for uniformity (Fig. 1a);

(ii) *Coconut coir*—extracted from coconut husks, dried, and ground to a powdery form (Fig. 1b);

Fig. 1: Constituents of composite bars.
(a): Sieved sawdust; **(b):** Extracted coir fibre;
(c): Epochem 105 epoxy resin; **(d):** MEKP catalyst.

(iii) *Epochem 105* clear epoxy resin (Part A) as the matrix (Fig. 1c);

(iv) *Methyl ethyl ketone peroxide (MEKP)* as a catalyst (Fig. 1d); and

(v) *Cobalt accelerator* to reduce curing time.

Wooden moulds (four beams arranged parallel with 2-inch spacing, clamped and waxed) were used to shape the composite bars.

Manufacturing Process

Sawdust and ground coconut coir were mixed with epoxy resin, MEKP catalyst, and cobalt accelerator at the specified proportions. Four composite bar specimens were cast:

- ***Sample 1*** (Equal fibre blend: 65% resin, 15% sawdust, 15% coir);
- ***Sample 2*** (Coir-dominant: 65% resin, 25% coir, 10% sawdust);
- ***Sample 3*** (Sawdust-dominant: 65% resin, 25% sawdust, 10% coir);
- ***Sample 4*** (High-fibre: 60% resin, 20% sawdust, 20% coir).

After curing, the bars were demoulded and cut to specimen dimensions per ASTM standards. The four fabricated composite bar specimens are shown in Fig.2.

Fig. 2: Fabricated composite bar specimens – Sample 1, Sample 2, Sample 3, and Sample 4.

Testing Equipment and Methods

Three characterisation methods were employed, each described with the corresponding equipment shown below.

Universal Testing Machine (Tensile Strength)

Tensile specimens were prepared per ASTM D638 with a gauge length of 50 mm. The specimen was clamped between the jaws of the UTM and loaded at a constant crosshead speed until fracture (Fig. 3).

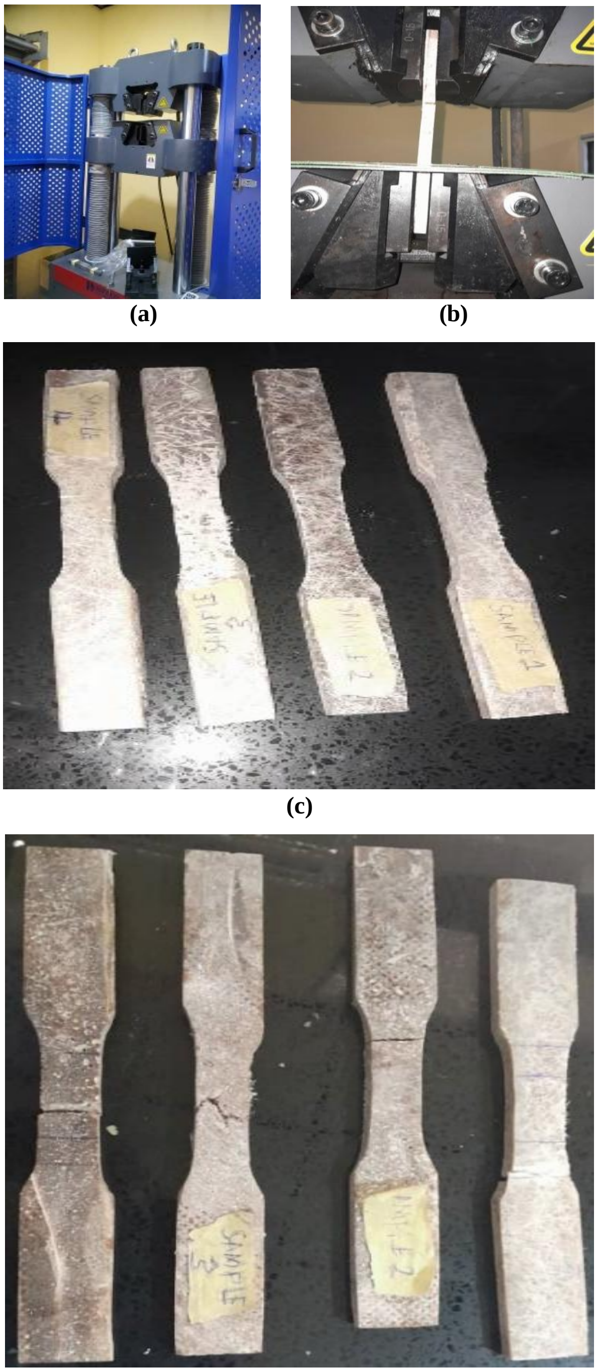

(a) (b) (c) (d)

Fig. 3: Tensile testing of specimens.
(a): Universal testing machine; **(b):** Specimen mounted for tensile test; **(c):** Tensile specimens prepared for testing; **(d):** Fractured specimens after tensile testing.

Charpy Impact Testing Machine

Impact specimens (10 × 10 × 55 mm) were prepared per ASTM E23. The pendulum hammer was raised to a specified height and released to strike the notched specimen, and the absorbed energy was recorded in joules (Fig. 4).

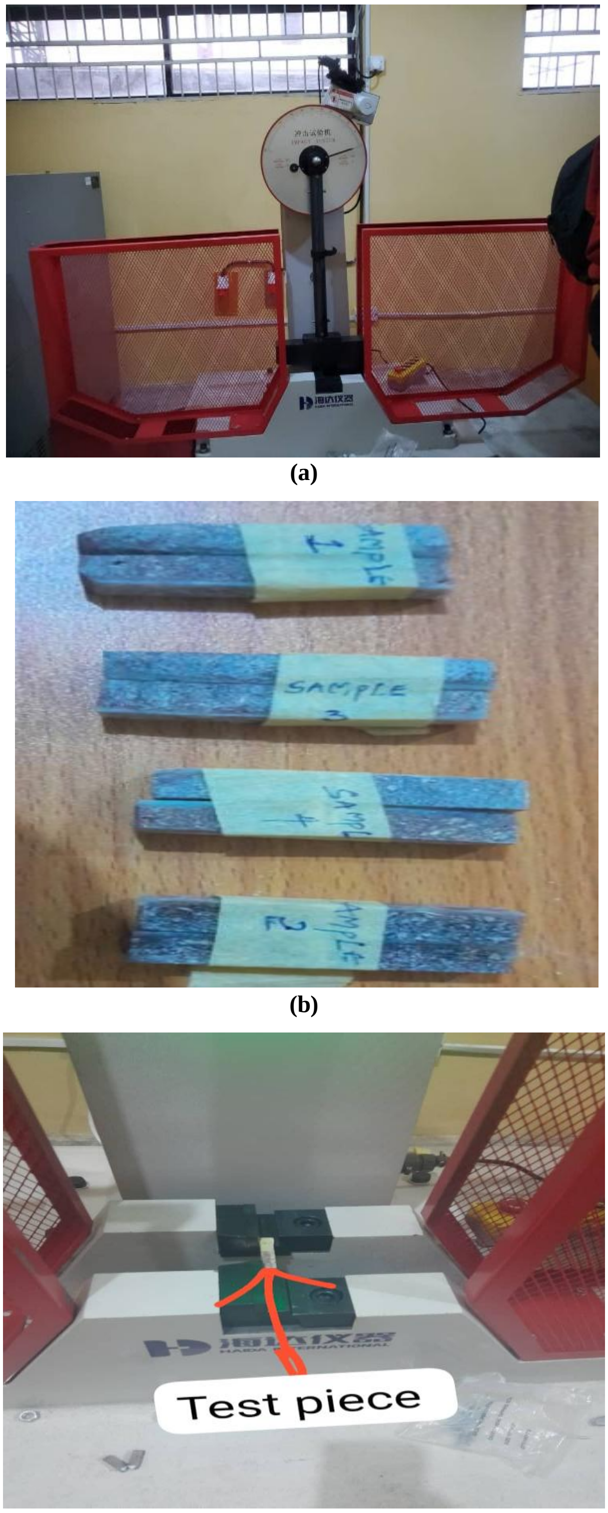

(a) (b) (c)

Fig. 4: Impact testing of specimens.
(a): Charpy testing machine; **(b):** Specimen placed for impact test; **(c):** Broken specimens after Charpy impact testing.

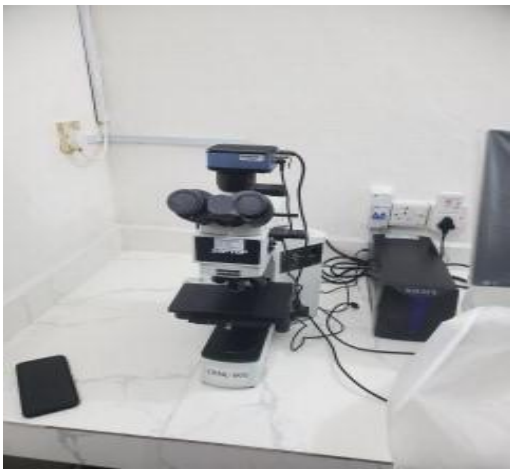

(a)

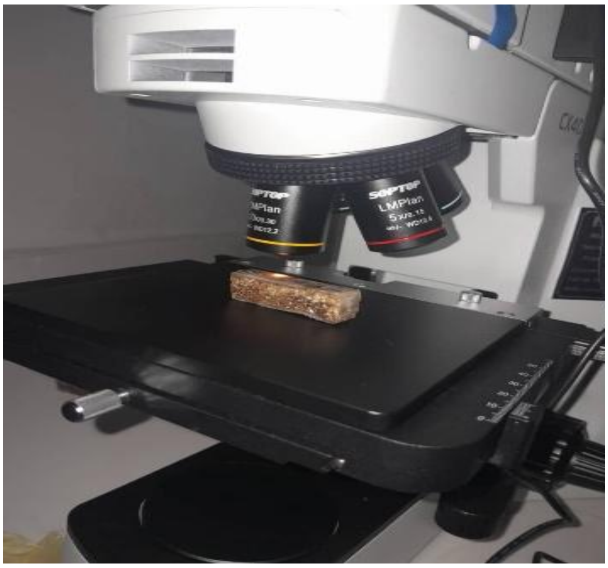

(b)

Fig. 5: Microstructural analysis of composite bars.
(a): Metallography microscope;
(b): Specimen on microscope stage.

Metallography Microscope (Microstructural Analysis)

Microstructural analysis was performed using a metallography microscope per ASTM E562 at magnifications of 100X and 200X. Specimens were polished and placed on the microscope stage for pre- and post-test examination (Fig. 5).

Analytical Methods

Tensile Strength (σ): Evaluated as the maximum stress under tension (Uesaka *et al.*, 2025):

$$\sigma = F / A \quad (1)$$

where, σ = tensile strength (MPa),
F = maximum applied force (N),
A = cross-sectional area (mm²).

Compressive Strength: Measures the maximum stress under compression (Uesaka *et al.*, 2025):

$$\sigma = Fc / A \quad (2)$$

where, Fc = maximum compressive force (N),
A = cross-sectional area (mm²).

Young's Modulus (E): Measures the stiffness of the composite (Uesaka *et al.*, 2025):

$$E = \sigma / \varepsilon \quad (3)$$

where, E = Young's modulus (MPa),
ε = strain (ΔL/L).

Impact Strength: Measured using the Charpy test as energy absorbed per unit area (Uesaka *et al.*, 2025):

$$\text{Impact Strength} = E / A \quad (4)$$

where, E = energy absorbed (J),
A = cross-sectional area at notch (mm²).

Fibre Volume Fraction (V_f): Determines the proportion of fibres in the composite (Thébault *et al.*, 2024):

$$V_f = V_{fiber} / V_{total} \quad (5)$$

where, V_{fiber} = fibre volume (m³),
V_{total} = total composite volume (m³).

RESULTS AND DISCUSSION

Result of Tensile Test Experimentation

The detailed tensile test data for all four specimens are presented in Table 1.

Result of Tensile Test Sample 1 Equal Fibre Blend

The stress–time graph for Sample 1 (Fig. 6a) illustrates a linear elastic phase reaching the yield strength (ReH) of 9 MPa, followed by a nonlinear phase peaking at the ultimate tensile strength (Rm) of 19 MPa at approximately 48 seconds. The sharp drop after Rm indicates brittle fracture, consistent with the 1.50% elongation. The balanced reinforcement provides a moderate yield–to–UTS ratio, reflecting the complementary contributions of both fibres.

Result of Tensile Test Sample 2 Coir-Dominant Hybrid

The stress–time curve for Sample 2 (Fig. 6b) rises steeply and linearly, reaching ReH of 12 MPa—the highest yield strength among all specimens—and Rm of 19 MPa at approximately

Table 1: Tensile test report.

Specimen	Width (mm)	Thickness (mm)	Area (mm²)	Max Load (kN)	UTS (MPa)	Yield (MPa)	Elongation (%)
Sample 1	19.01	11.85	225.27	4.28	19	9	1.50
Sample 2	18.67	10.15	189.50	3.60	19	12	1.50
Sample 3	19.01	11.80	224.32	2.68	12	7	1.50
Sample 4	18.60	13.53	251.66	2.86	11	5	1.50

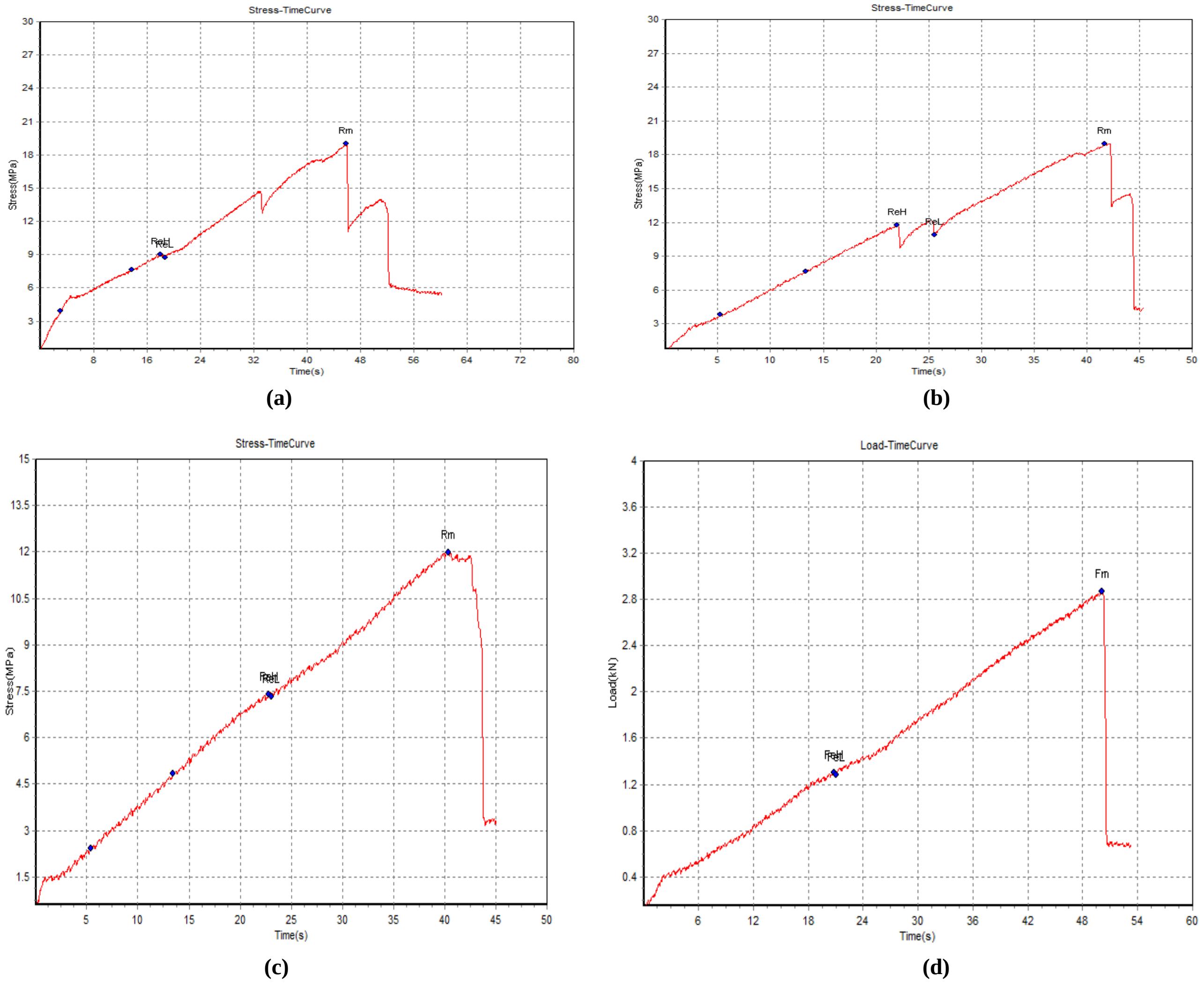

Fig. 6: (a): Stress-Time curve for Sample 1 (Equal Fibre Blend); **(b):** Stress-Time curve for Sample 2 (Coir-Dominant Hybrid); **(c):** Stress-Time curve for Sample 3 (Sawdust-Dominant Hybrid); **(d):** Load-Time curve for Sample 4 (High-Fibre Content).

42 seconds. The higher coir content enhances tensile reinforcement due to the coconut fibre's inherent tensile properties and lignin content. The abrupt post-peak drop confirms brittle fracture typical of natural fibre composites.

Result of Tensile Test Sample 3 Sawdust-Dominant Hybrid

With a cross-sectional area of 224.32 mm² and a maximum load of 2.68 kN, the graph (Fig. 6c) shows a linear elastic phase to ReH of 7 MPa, peaking at an Rm of 12 MPa—the lowest ultimate tensile strength recorded. This indicates that higher sawdust content compromises tensile performance, attributed to weaker fibre-matrix bonding from sawdust's irregular particulate morphology. The sharp post-peak drop at approximately 40 seconds reflects brittle fracture.

Result of Tensile Test Sample 4 High-Fibre Content

With a cross-sectional area of 251.66 mm², the load increases linearly to approximately 3 kN, with a yield load (FeH) of around 1.4 kN and a maximum load (Fm) of 2.86 kN at approximately 50 seconds (Fig. 6d). The UTS of 11 MPa is the lowest among all specimens, suggesting that inconsistent fibre–matrix adhesion at higher total fibre content limits mechanical performance.

Result of Charpy Impact Test Experimentation

Table 2 presents the complete Charpy impact test data for all specimens tested at ambient temperature (25°C).

The absorbed energy ranged from 1.15 J (Sample 2, Trial A) to 3.00 J (Samples 1 and 4, Trial A). Sample 1 (equal fibre

Table 2: Charpy impact test report.

Specimen	Dimension (mm)	Area (cm²)	Temp. (°C)	Energy A (J)	Energy B (J)	Avg. Energy (J)
Sample 1	10×10×55	0.8	25	3.00	1.35	2.18
Sample 2	10×10×55	0.8	25	1.15	1.25	1.20
Sample 3	10×10×55	0.8	25	1.50	1.82	1.66
Sample 4	10×10×55	0.8	25	3.00	1.25	2.13

blend) achieved the highest average energy absorption (2.18 J), indicating effective energy dissipation through balanced fibre–matrix interactions. Sample 2 (coir-dominant) recorded the lowest average (1.20 J) despite its superior tensile strength, revealing a trade-off between tensile and impact properties that is consistent with literature on natural fibre composites [9]. Sample 4 performed comparably to Sample 1 in impact resistance (2.13 J), indicating that higher total fibre content can enhance toughness even when tensile properties are reduced. The brittle fracture observed in post-impact specimens (Fig. 8h) aligns with the low elongation (1.50%) from tensile tests.

Result of Microstructural Analysis

Microstructural Analysis Sample 1 Equal Fibre Blend

The pre-test micrograph at 200X magnification (Fig. 8a) reveals coir fibres that are partially aligned as a result of the hand lay-up process, with evidence of resin penetration into the fibre's cellular structure, indicating mechanical interlock that supports initial load transfer. The post-test micrograph (Fig. 8b) reveals extensive fibre bond breakage and matrix cracking originating at the notch tip, propagating through the brittle epoxy, consistent with the high average impact energy of 2.18 J, indicating energy dissipation through fibre pull-out.

Microstructural Analysis Sample 2 Coir-Dominant Hybrid

The pre-test image (Fig. 8c) highlights the presence of irregularly shaped sawdust particles dispersed throughout the matrix, contributing to the composite's bulk properties by filling voids. Minor voids and gaps are visible, stemming from incomplete resin mixing during hand lay-up. The post-test image (Fig. 8d) exposes pronounced delamination and expanded voids, particularly in areas with uneven resin distribution, facilitating crack propagation under impact and correlating with the low average energy absorption of 1.20 J.

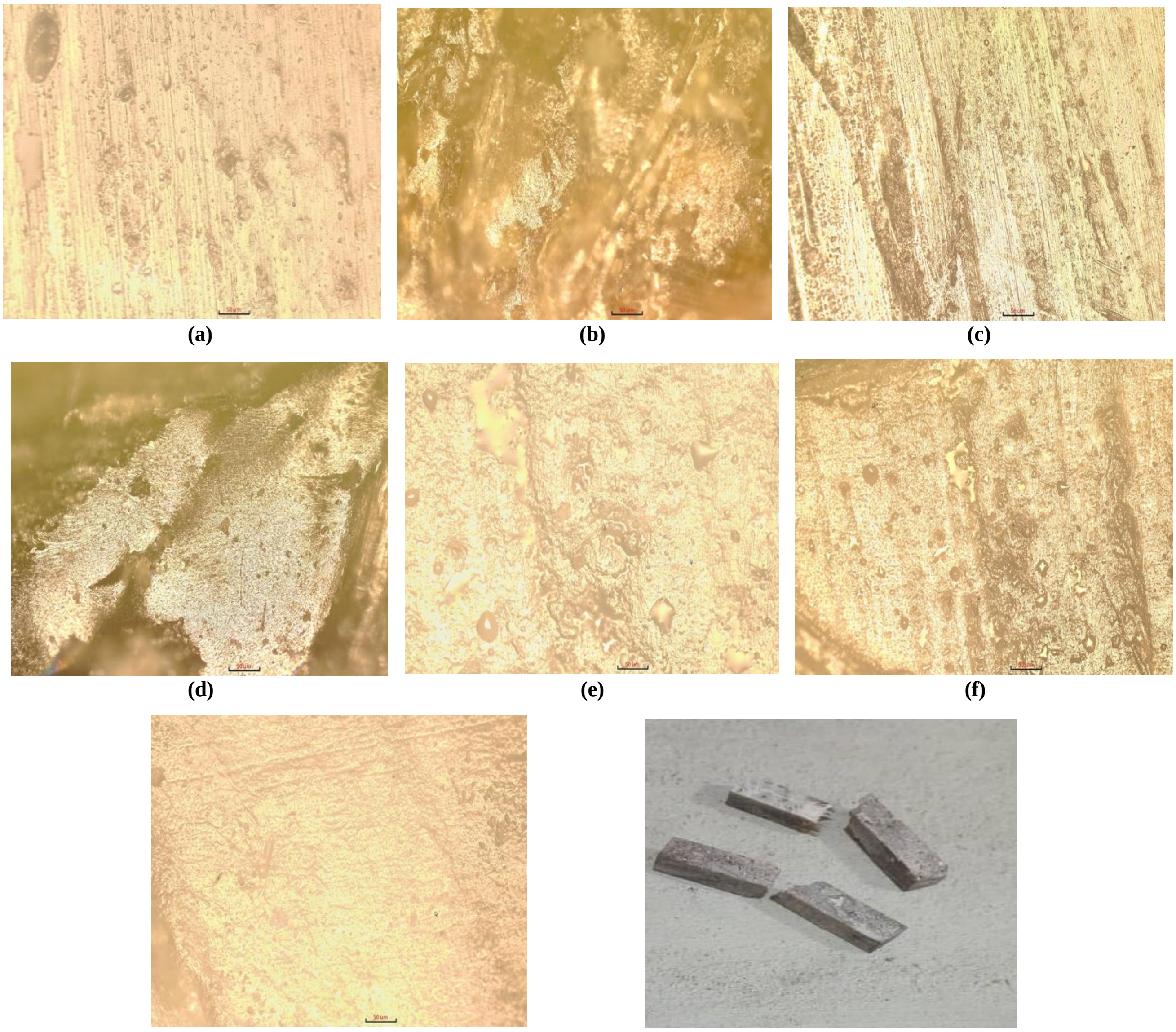

(a) (b) (c) (d) (e) (f) (g) (h)

Fig. 8: Microstructural analysis samples. **(a):** Sample 1 pre-test at 200X; **(b):** Sample 1 post-test at 200X; **(c):** Sample 2 pre-test at 100X; **(d):** Sample 2 post-test at 100X; **(e):** Sample 3 pre-test at 200X; **(f):** Sample 3 post-test at 200X; **(g):** Sample 4 pre-test at 100X; **(h):** Sample 4 broken pieces after impact.

Microstructural Analysis Sample 3 Sawdust-Dominant Hybrid

The pre-test micrograph (Fig. 8e) displays a heterogeneous distribution of coir fibres identifiable by their porous, cellulose-rich structure embedded within the epoxy matrix. The post-test micrograph (Fig. 8f), which recorded the highest single-trial impact energy of 1.82 J, shows increased fibre fracture alongside bond breakage, suggesting better interfacial bonding or alignment due to more uniform distribution of coir fibres and sawdust particles. The sawdust-dominant composition, while limiting tensile performance, appears to support moderate impact energy dissipation through increased fibre fracture mechanisms.

Microstructural Analysis Sample 4 High-Fibre Content

The pre-test image (Fig. 8g) reveals variability in the fibre–matrix interface, with some regions showing tight bonding and others displaying loose contact, particularly around sawdust particles, suggesting suboptimal interfacial adhesion from untreated fibres. The post-test image shows significant particle debonding with cavities where sawdust particles have detached from the matrix, correlating with reduced energy absorption. Fibre bond breakage is a dominant feature, and delamination between layers is also evident, consistent with the lower tensile strength (11 MPa) recorded.

Comparison with Literature

The tensile strengths obtained (11–19 MPa) are comparable to values reported for natural fibre composites. Bui *et al.* (2020) reported untreated coir tensile strengths of 15–25 MPa, while Hasan *et al.* (2020) found values of 18–27 MPa. The current results are lower than synthetic composites but competitive with other natural fibre systems, and consistent with Oladele *et al.* (2020), who reported 25 MPa for polyester-matrix hybrid sawdust–coir composites. The slight difference may be attributed to the epoxy matrix properties and the absence of fibre surface treatment in the current study. The results confirm the viability of sawdust–coir epoxy composite bars for low-cost, eco-friendly structural applications.

CONCLUSION

This study successfully demonstrated that sawdust and coconut coir can be effectively utilised as co-reinforcement materials in epoxy composite bars, offering a sustainable alternative to synthetic fibres. Tensile testing yielded ultimate strengths of 11–19 MPa with 1.50% elongation and abrupt post-peak failures, characterising the brittle nature of natural fibre–reinforced epoxy composites.

The coir-dominant composite (Sample 2) achieved the highest ultimate tensile strength (19 MPa) and yield strength (12 MPa), confirming coir's dominant tensile reinforcing role due to its high lignin content and tensile properties.

Charpy impact testing demonstrated that the equal fibre blend (Sample 1) achieved the highest average energy absorption (2.18 J), reflecting effective energy dissipation through balanced fibre–matrix interactions, while the coir-dominant specimen showed the lowest impact resistance (1.20 J), revealing a tensile–impact trade-off. Microstructural analysis underscored the critical importance of uniform fibre distribution and effective resin penetration, with voids and particle debonding identified as key performance-limiting factors.

Overall, these novel hybrid sawdust/coir-epoxy composite bars show significant promise for sustainable structural applications in furniture, packaging, and low-cost construction, but require optimised fibre surface treatment and fabrication techniques to enhance reliability and achieve broader industrial adoption. The adoption of such eco-friendly products is vital for supporting sustainability objectives, as set forth by the United Nations Sustainable Development Goals (SDGs) (Farid *et al.*, 2026) and Millennium Development Goals (MDGs) (Garba and Abdullahi, 2026), and climate change actions, as articulated in the Paris Agreement (Deswal, 2025).

Acknowledgement

The authors would like to appreciate the efforts of CACTI Resources Nigeria Limited and the technical staff of the Department of Mechanical Engineering, Rivers State University, Port Harcourt, for their support throughout the experimental programme.

Grant Support Details

The funding for this research was provided by both authors of this publication.

Data Availability

The data could be made available on request from CACTI Resources Nigeria Limited.

Use of AI and AI-assisted Technologies

There was no use of artificial intelligence in the writing, analysis, and image generation. All images were generated from the different machines used in carrying out the tests.

Conflict of Interest

There is no conflict of interest whatsoever between the authors or the laboratory (CACTI Resources Nigeria Limited) where the mechanical tests were carried out.

Copyright Permissions

Both authors declare that all copyright permissions for all figures included in this article have been duly obtained, as the work is original and was carried out by both authors, and the laboratory where all mechanical tests were conducted is duly licensed.

REFERENCES

1) Ajiri, M.A., Edomwonyi-Otu, L. and Okieimen, F.E. (2024) 'Use of sawdust and coconut fibre as fluid loss control additives for water-based mud,' *J. Pet. Sci. Eng.*, 223, pp. 211–220.
2) Bui, T.T., Tran, V.T. and Nguyen, H.T (2020) 'Physical and mechanical properties of raw and treated coconut fibres for construction materials,' *J. Nat. Fibres*, 17(8), pp. 1123–1135.
3) Daniel, I.M. and Ishai, O. (2006) *Engineering mechanics of composite materials*. Oxford, U.K.: Oxford Univ. Press.
4) Deswal, P. (2025) 'Article 6 of the Paris Agreement: A comprehensive review of mechanisms, progress, and persistent challenges', *International Journal of Technology, Health and Sustainability*, 1(2), pp. 111-125. https://ijths.com/wp-content/uploads/IJTHS-010235.pdf

5) Farid, S., Razzaq, S. and Sajid, M. (2026) 'Impact of balanced use of fertilizer on crop production and its quality for human health', *International Journal of Technology, Health and Sustainability*, 2(1), pp. 29-38. https://ijths.com/wp-content/uploads/IJTHS-020143.pdf
6) Garba, A. and Abdullahi, M.G. (2026) 'Evaluation of climatic trends in Dass LGA, Bauchi State, Nigeria', *International Journal of Technology, Health and Sustainability*, 2(1), pp. 52-56. https://ijths.com/wp-content/uploads/IJTHS-020147.pdf
7) Gibson, R.F. (2016) *Principles of composite material mechanics*. Boca Raton, FL, USA: CRC Press.
8) Gurusamy, S., Kumar, R. and Prasad, V. (2024) 'Effect of fine powder loads on hybrid composites of Malabar Ironwood sawdust and COCO dust,' *Polym. Compos.*, 45(3), pp. 245–256.
9) Hasan, K.M.F., Horváth, P.G. and Alpár, T. (2020) 'Mechanical properties of coconut fibre-reinforced polymer composites,' *J. Reinf. Plast. Compos.*, 39(15), pp. 567–578.
10) Mallick, P.K. (2007) *Fiber-reinforced composites: Materials, manufacturing, and design*. Boca Raton, FL, USA: CRC Press.
11) Oladele, I.O., Okoro, A.M. and Adewuyi, B.O. (2020) 'Development and characterization of hybrid sawdust–coconut fibre composites in polyester matrix,' *J. Compos. Mater.*, 54(12), pp. 1567–1578.
12) Prakash, R., Anandh, S., Nachiar, S.S., *et al.* (2020) 'A study on mechanical and durability properties of coconut shell concrete using coconut fiber and sawdust,' *Mater. Sci. Eng.*, 912, 062068. DOI 10.1088/1757-899X/912/6/062068
13) Singh, A., Singh, N. and Khare, N. (2026) 'Eco-friendly synthesis and evaluation of silver nanoparticles (agnps) using *Azadirachta indica*: A greener approach to boosting antimicrobial power', *International Journal of Technology, Health and Sustainability*, 2(1), pp. 233-237. https://ijths.cFaridom/wp-content/uploads/IJTHS-020180.pdf
14) Soutis, C. (2005) 'Fibre reinforced composites in aircraft construction,' *Prog. Aerosp. Sci.*, 41(2), pp. 143–151.
15) Tawasil, M.R., Ibrahim, R. and Ahmad, Z. (2021) 'Coconut fibre and sawdust as green building materials: Physical and mechanical properties of hybrid particleboards,' *Constr. Build. Mater.*, 271, pp. 121–129.
16) Thébault, F., Clément, A, Fréour, S., *et al.* (2024) 'Comparison of fiber volume fraction measurement methods from composite micrographs,' *Composites Science and Technology*, 282, 111689. https://doi.org/10.1016/j.compscitech.2026.111689.
17) Uchendu, I.F., Akaninwor, G.C. and Nna, G. (2026) 'Evaluate the performance of biodegradable composites made from lime and mango peel', *International Journal of Technology, Health and Sustainability*, 2(1), pp. 195-200. https://ijths.com/wp-content/uploads/IJTHS-020171.pdf
18) Uesaka, M., Onizawa, K., Kasahara, N., *et al.* (2025) 'Strength of materials and structural mechanics.' In: *Nuclear Structural Engineering*. Singapore: Springer Nature. https://doi.org/10.1007/978-981-97-3519-8_2